Electronic Supplementary Material (ESI) for Physical Chemistry Chemical Physics.

Oxidation of $NO^{\bullet}$ by the small oxygen species HO_2^- and $O_2^{\bullet-}$: The role of negative charge, electronic spin and water solvation.

Mauritz Johan Ryding[1], *Israel Fernández*[2] *and Einar Uggerud*[1,*]

[1] Mass Spectrometry Laboratory and Centre of Theoretical and Computational Chemistry, Department of Chemistry, University of Oslo, P.O. Box 1033 Blindern, NO-0315 Oslo, Norway

[2] Departamento de Química Orgánica I, Facultad de Ciencias Químicas, Universidad Complutense de Madrid, 28040-Madrid, Spain.

* einar.uggerud@kjemi.uio.no

Supplementary Information

Detailed experimental data

Figures S1 and S2 contains the experimental data of Figures 1 and 5, respectively; however, here the data is displayed for each cluster size as a function of centre-of-mass collision energy. Figures S1 and S2 also shows all the products (*i.e.* also the neutral reaction products) of the nominal reactions $HO_2^-(H_2O)_n + NO^\bullet$ and $O_2^{\bullet-}(H_2O)_n + NO^\bullet$; furthermore, different degrees of water loss associated with a reaction is treated as a separate reaction channel.

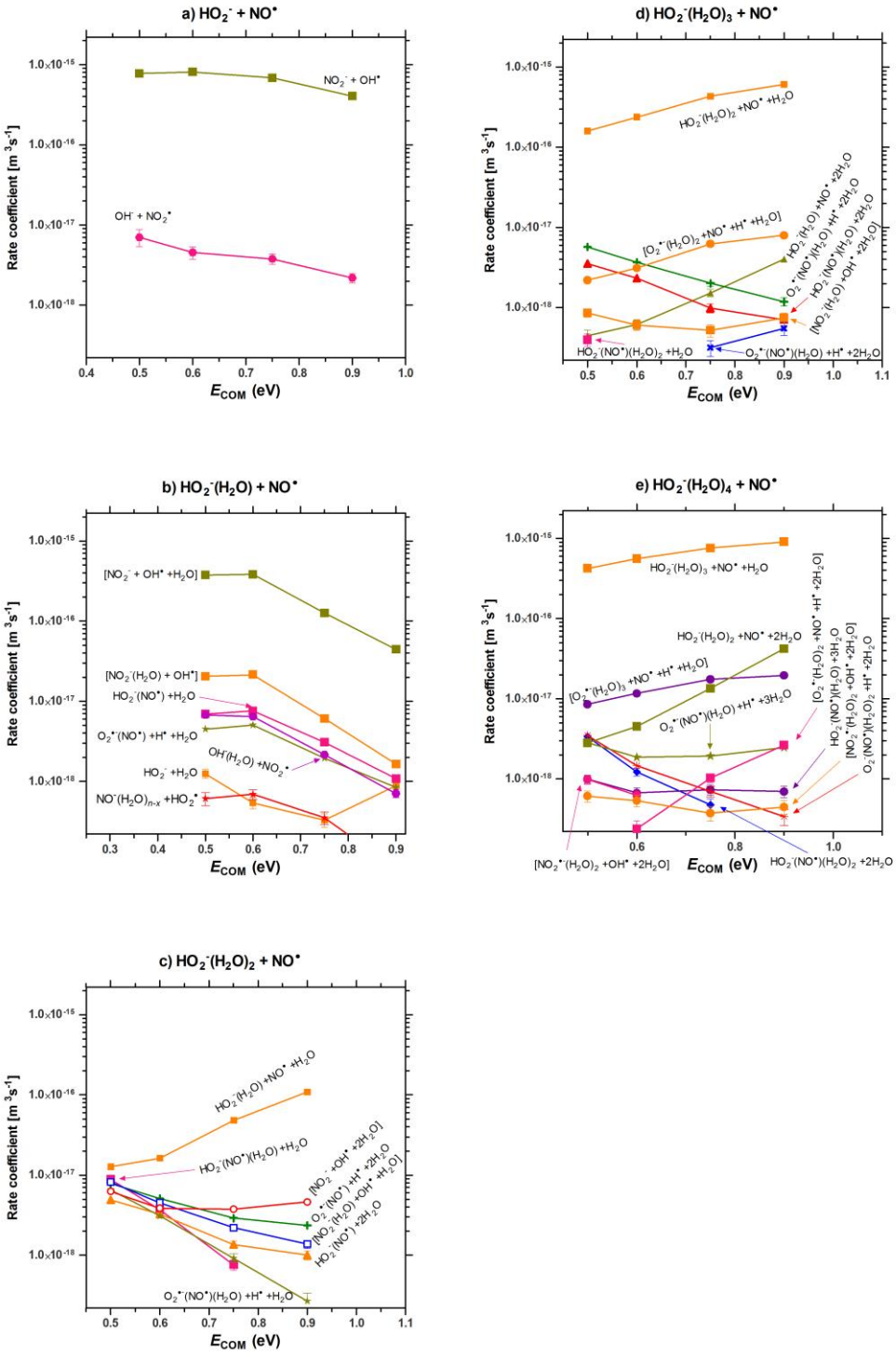

Figure S1. Reaction rate coefficients for $HO_2^-(H_2O)_n$ + NO• leading to the indicated, nominal, product pairs. The data is given for different values of *n* (panels a–e) and for different values of centre-of-mass collision energy (abscissa). The absolute values of the rate coefficients are expected to be accurate within 25%. Error bars represent one SD due to count statistics. Products in square brackets can also be the result of contaminants.

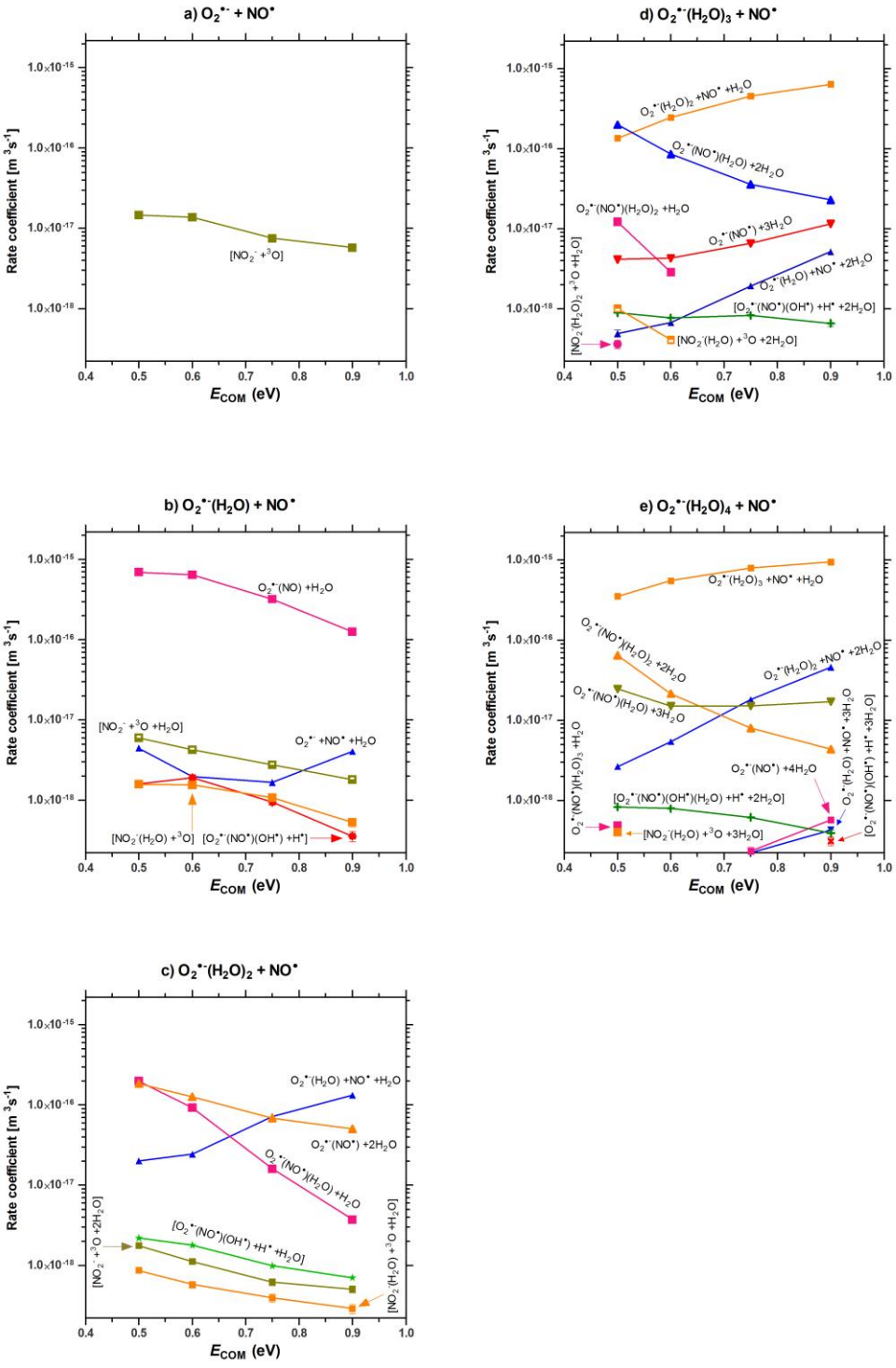

Figure S2. Reaction rate coefficients for $O_2^{\bullet-}(H_2O)_n$ + NO$^\bullet$ leading to the indicated, nominal, product pairs. The data is given for different values of *n* (panels a–e) and for different values of centre-of-mass collision energy (abscissa). The absolute values of the rate coefficients are expected to be accurate within 25%. Error bars represent one SD due to count statistics. Products in square brackets can also be the result of contaminants.

$NO_2^\bullet$ contamination

$NO_2^\bullet$ is present as a contamination in the $NO^\bullet$ gas used, and it is important to try and establish the degree of the impurity and to what extent it will influence the results. In order to remove $NO_2^\bullet$ from $NO^\bullet$, the gas was led through a cold trap prior to entering the collision cell of the mass spectrometer; the cold trap was kept at approximately −114 °C by means of a cooling bath of liquid nitrogen and ethanol. This allows the removal of $NO_2^\bullet$, but not $NO^\bullet$, based on their respective boiling points of 21.15 and −151.74 °C.[1] It is possible that $NO^\bullet$ will form $NO_2^\bullet$ in reactions with adsorbed oxygen on the inner surface of the tubing leading from the cold trap into the collision cell.

We will consider the NO_2^- formation from $O_2^{\bullet-}$ in Figure 5. In order to arrive at an upper limit estimate for the degree of $NO_2^\bullet$ contamination in the experiments, we will make the following assumptions. The formation of NO_2^- starting from $O_2^{\bullet-}(H_2O)$ is assumed to occur solely due to a charge transfer to the contaminant $NO_2^\bullet$ (reaction 17). Furthermore we assume that this reaction have a reaction cross section that is not lower than that of reaction 15, $O_2^{\bullet-}(H_2O) + NO^\bullet \rightarrow O_2^{\bullet-}(NO^\bullet)(H_2O)_{1-x} + xH_2O$, which is the main reaction of superoxide clusters with $NO^\bullet$. A direct comparison of reaction 15 to the presumed reaction 17 in Figure 5 gives an upper limit for the $NO_2^\bullet$ contamination of 0.88%. As the number of water molecules on the superoxide ion increase, the reaction rate coefficient of both reactions can be seen to decrease while the ratio is kept more or less constant (parallel lines in Figure 5). It should be pointed out that we have here ignored the other two reactions detected for the superoxide clusters, although we expect them to not greatly influence the estimate.

The ratio of $NO^\bullet$ to $NO_2^\bullet$ being 0.9911:0.0088 is actually greater than the purity of the $NO^\bullet$ gas used (99.5%), which would indicate that the cold trap has no effect. A separate measurement was performed comparing the effect on NO_2^- formation starting from superoxide–water clusters, with

and without the cold trap in place; the effect is shown in Figure S3. It was observed that for $O_2^{\bullet-}$ the introduction of the cold trap lowered the observed NO_2^- formation to 37% of the value obtained without the cold trap; the corresponding figure for $O_2^{\bullet-}(H_2O)$ was 27%. From this we can conclude that the $NO_2^\bullet$ formation occurring due to adsorbed oxygen in the gas tubing is rather efficient.

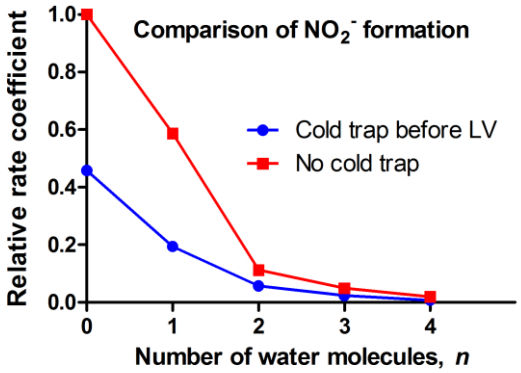

Figure S3. Comparison of NO_2^- formation from superoxide–water clusters in measurements with and without a cold trap in place, expressed on a relative scale. The data is given for a centre-of-mass collision energy of 0.6 eV and different cluster sizes *n*.

Computational results for $HO_2^\bullet(H_2O)$

As mentioned in the main text, solvation of the reactant HO_2^- disperses some of the negative charge onto the water molecule, which hampers electron transfer, which in turn is a major driving force for the oxidation reaction. In order to further test the assumption that the oxidation reactions is inhibited by hydration we performed a set of calculations for the electrically neutral reaction $HO_2^\bullet(H_2O)$ + $NO^\bullet$, the results are presented in Figure S4. The effect of hydration is found to be smaller for the neutral $HO_2^\bullet(H_2O)$ compared to the anionic $HO_2^-(H_2O)$ (Figure 3). However, also for the neutral case, the overall oxidation reaction (*i.e.* $NO^\bullet \rightarrow NO_2^\bullet$) of the hydrated reactant is less exothermic compared to the naked reactant (by 16 kJ mol^{-1}). As seen, the first transition state for $HO_2^\bullet(H_2O)$ + $NO^\bullet$ is only 5.3 kJ mol^{-1} higher compared to that of the naked $HO_2^\bullet$ (Figure 4, the corresponding activation barriers with respect to the separate reactants are 170.4 kJ mol^{-1} vs 165.1 kJ mol^{-1} for the

processes involving **bTS1w** and **bTS1**, respectively). We also note that the central elementary oxidation step (**bINT1w** → **bINT2w**) is exergonic by 5.5 kJ mol^{-1} for the hydrated radical, while it is exergonic by 18.2 kJ mol^{-1} for the bare radical (**bINT1** → **bINT2** in Figure 4), providing a rationale for the slightly higher barrier in the hydrated case. Finally we note by comparison of Figure 4 and Figure S4 that the presence of a water molecule enables the formation of monohydrated nitric acid in the latter case; while this reaction is overall exergonic (−153.3 kJ mol^{-1}), it still has the substantial barrier of **bTS1w** in the initial phase.

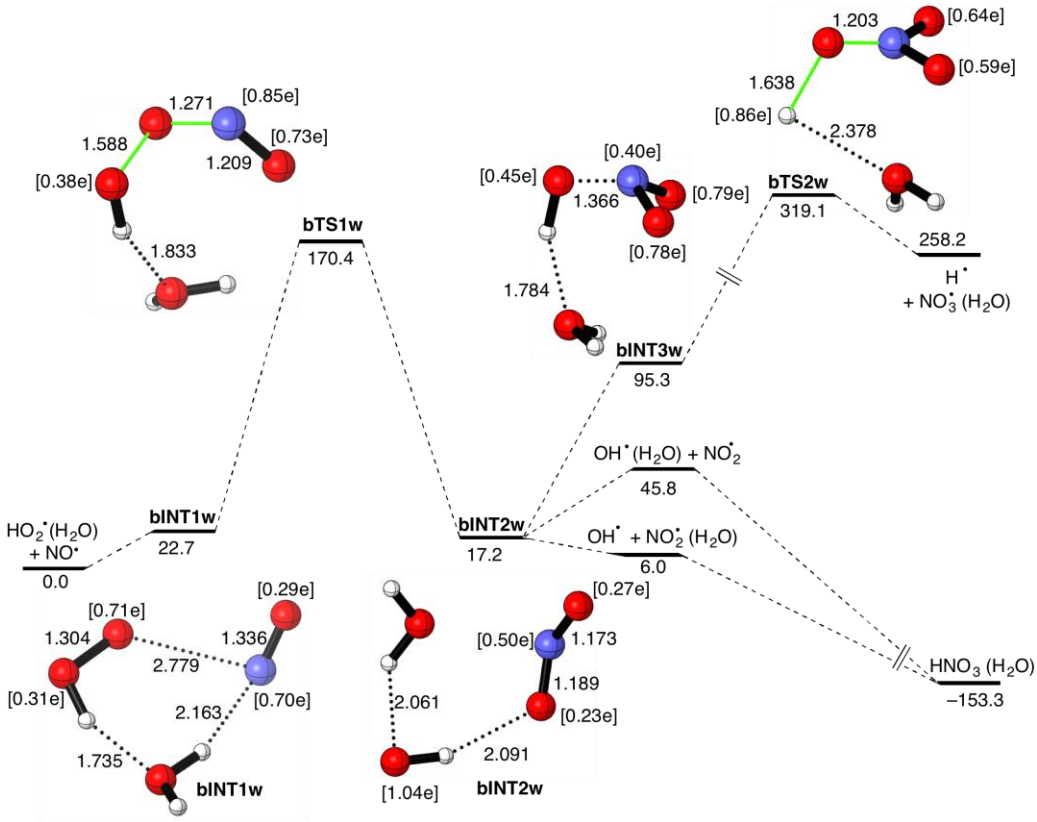

Figure S4. Computed potential energy profile (triplet electronic state) of the reaction between $HO_2^{\bullet}$ (H_2O) and $NO^{\bullet}$. Bond distances and relative free energies are given in angstroms and kJ mol^{-1}, respectively. Computed spin densities are given in square brackets. All data have been computed at the uM06-2X/6-311+G(d,p) level.

Relaxed scans for the formation of HOONO from HO_2^- and $NO^\bullet$

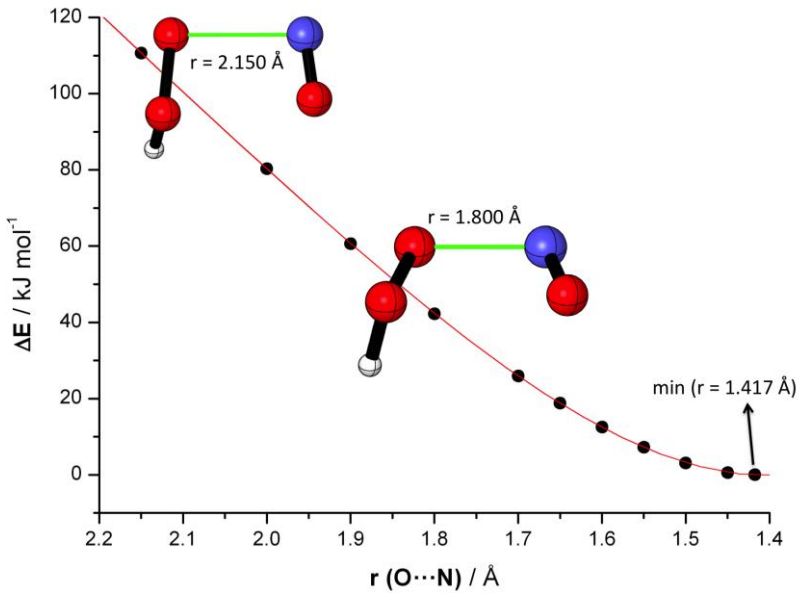

Figure S5. Fully relaxed scans performed for the formation of HOONO from HO_2^- and $NO^\bullet$ on the singlet hypersurface. The energies and geometries were computed at different HOO···NO distances, denoted as *r*. All data have been computed at the M06-2X/6-311+G(d,p) level.

Computational results for O_2

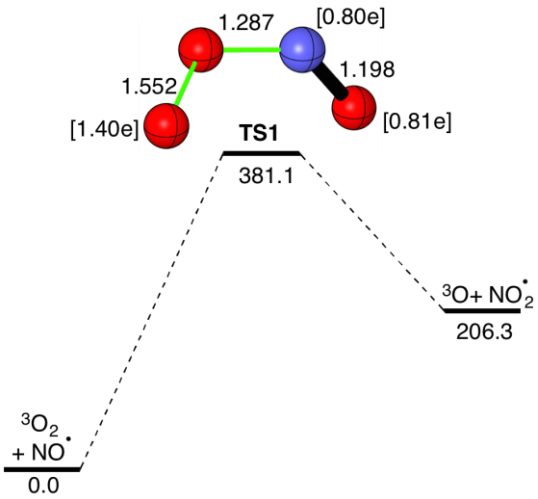

Figure S6. Computed profile for the reaction between $^3O_2$ and $NO^{\bullet}$ (quartet hypersurface). Bond distances and relative free energies are given in angstroms and kJ mol^{-1}, respectively. Computed spin densities are given in square brackets. All data have been computed at the uM06-2X/6-311+G(d,p) level.

For the sake of completeness, we have also included computational results for the reaction between $^3O_2$ and $NO^{\bullet}$ to give ^3O + $NO_2^{\bullet}$ (Figure S6). Not surprisingly, the reaction is both strongly endothermic and has a high barrier in agreement with Siegbahn.[2] The gain of forming one N–O bond does by no means counterbalance the cost of breaking the strong O–O bond, and there is no extra driving force in this situation to facilitate oxidation — neither by electron transfer to give NO_2^- nor by spin pairing.

Collisional cross-sections and rates of reactions with $NO^{\bullet}$ and $NO_2^{\bullet}$, kinetic considerations

Formation of the products, NO_2^- and OH^-, show decreasing reaction rates with increasing collision energy (Figure S1a); they decrease by 50% and 70% when increasing the centre-of-mass collision energy from 0.5 eV to 0.9 eV, respectively. The cross section for a collision between an ion and a dipole is velocity dependent, and can be described by average dipole orientation (ADO) theory or

hard sphere deflection (HSD) theory.[3-6] We estimated the collision rate coefficient for HO_2^- (and $O_2^{\bullet-}$) colliding with $NO^\bullet$ and $NO_2^\bullet$ using these theories and find that the relative ion–gas velocity has a negligible effect.[7, 8] In essence, there are two contributions to the calculated rate coefficients, namely, one coming from the polarization of the neutral molecule and one from the ion–permanent dipole interaction. In the ADO rate coefficient, the former contribution is velocity independent while the latter contribution is inversely proportional to the velocity. The polarizability contribution dominates the ADO rate coefficients for $NO^\bullet$ and $NO_2^\bullet$ already at velocities corresponding to gases at room temperature. The calculated collision rate coefficients are essentially the same for HO_2^- or $O_2^{\bullet-}$, but varies depending upon the neutral molecule being $NO^\bullet$ or $NO_2^\bullet$; they are approximately 7.8×10^{-16} m^3s^{-1} for $NO^\bullet$ and 1.0×10^{-15} m^3s^{-1} for $NO_2^\bullet$ over the current energy range of 0.5–0.9 eV. This collision rate is in reasonable agreement with a rate coefficient for charge transfer from superoxide to $NO_2^\bullet$—ranging from 1.8×10^{-15} m^3s^{-1} to 1.9×10^{-15} m^3s^{-1} for 5000–10 000 K (0.43–0.86 eV)—that Rutherford and Turner reported based on extrapolation from high eV experiments.[9] It is also in good agreement with the absolute reaction rate coefficient for reaction 3a which, using the experimental data for 0.6 eV collision energy and an approximate pressure of 2.3×10^{-4} mbar, was calculated to be 8.1×10^{-16} m^3s^{-1}.

Without reading too much into a comparison of these theoretical collision rates and our experimental reaction rates, we would like to highlight some factors that might be the origin of the perceived discrepancy of an experimentally determined rate coefficient that is collision energy–dependent, and a theoretically predicted rate coefficient that is velocity-independent. First and foremost, the comparison involves—as just mentioned—a collision rate coefficient and a reaction rate coefficient. It is not certain that all collisions will lead to reaction, and we can envision a velocity/energy dependent sticking factor (nominal ion velocities are about 2500 ms^{-1} at 0.5 eV and 3350 ms^{-1} at 0.9 eV). Furthermore, higher collision energy can cause a higher translational energy of the product ion

as it leaves the reaction complex; this might deflect it enough that it is not properly focused by the ion optics in the instrument and thereby lead to lower detection efficiency. In addition, higher collision energies mean more energetic, and therefore more short-lived, reaction complexes which might inhibit the reaction. It should be pointed out that for reactions occurring at these low pressures the absence of a third body to help stabilize formed products can result in dissociation back to the reactants.

As hydration of the reactant ions increases, things will change. For one, the relative ion–gas velocity will decrease given the same collision energy in the centre-of-mass frame. Secondly, the presence of water molecules and the extra degrees-of-freedom they introduce should increase the lifetime of energetic reaction complexes, as well as help stabilize any products formed by providing a means for the product to rid itself of excess energy by evaporation. However, the shielding of the core ion by H_2O (solvation shell) will typically decrease the reaction rate as it is necessary to dissolve the ion prior to reaction; for this reason, higher collision energy is often beneficial to help crossing the reaction barrier.

References

1. "Physical Constants of Inorganic Compounds" in *CRC Handbook of Chemistry and physics, internet version 2006*, ed. D. R. Lide, Taylor and Francis, Boca Raton, FL, USA, 86th edn., 2006.
2. P. E. M. Siegbahn, *J. Comput. Chem.*, 1985, **6**, 182-188.
3. T. Su and M. T. Bowers, *Int. J. Mass Spectrom. Ion Phys.*, 1973, **12**, 347-356.
4. G. Kummerlowe and M. K. Beyer, *Int. J. Mass Spectrom.*, 2005, **244**, 84-90.
5. T. Su and M. T. Bowers, *J. Chem. Phys.*, 1973, **58**, 3027-3037.
6. G. Gioumousis and D. P. Stevenson, *J. Chem. Phys.*, 1958, **29**, 294-299.
7. T. M. Miller, in *CRC Handbook of Chemistry and physics, internet version 2006*, ed. D. R. Lide, Taylor and Francis, Boca Raton, FL, USA, 86th edn., 2006.
8. "Dipole Moments" in *CRC Handbook of Chemistry and physics, internet version 2006*, ed. D. R. Lide, Taylor and Francis, Boca Raton, FL, USA, 86th edn., 2006.
9. J. A. Rutherford and B. R. Turner, *J. Geophys. Res.*, 1967, **72**, 3795-3800.

Quantum Chemical Computation data

Cartesian coordinates (in Å) and total energies (in a. u., ZPVE included) of all the stationary points discussed in the text. All calculations have been performed at the M06-2X/6-311+G(d,p) level.

HO_2^-: E= -150.911043

O	0.055460000	-0.687460000	0.000000000
H	-0.887367000	-0.865164000	0.000000000
O	0.055460000	0.795605000	0.000000000

NO·: E= -129.875522

O	0.000000000	0.000000000	0.531209000
N	0.000000000	0.000000000	-0.607096000

aINT1: E= -280.824372

O	-1.209903000	-0.595893000	-0.000151000
H	0.424401000	-1.082100000	-0.000111000
O	1.260644000	-0.553827000	0.000151000
O	0.705293000	0.750199000	-0.000217000
N	-0.924668000	0.611181000	0.000264000

aTS1: E= -280.819266

O	-0.461618000	0.749751000	-0.215026000
O	-1.397997000	-0.450791000	0.110990000
H	-0.747858000	-1.134382000	-0.117717000
O	1.243432000	-0.607528000	-0.118902000
N	0.811047000	0.514704000	0.271602000

aINT2: E= -280.877416

O	1.045991000	0.963566000	0.000582000
O	-2.190795000	0.248115000	-0.000364000
H	-1.254692000	-0.123450000	0.001152000
O	0.213642000	-0.974742000	0.000754000
N	1.243427000	-0.253151000	-0.001275000

aINT3: E= -280.865779

N	0.190831000	0.022662000	-0.242616000
O	0.282664000	1.250932000	0.072925000
O	1.018006000	-0.850272000	0.088498000
O	-1.257760000	-0.469551000	0.036113000
H	-1.679095000	0.392490000	0.118023000

aTS2: E= -280.820297

N	-0.082186000	-0.000007000	-0.062650000
O	-0.671645000	-1.086397000	0.041742000
O	-0.673271000	1.085459000	0.041911000
O	1.192983000	0.000930000	-0.172945000
H	1.790761000	0.000113000	1.152889000

$HO_2^-(H_2O)$: E= -227.354845

O	0.626150000	0.785396000	0.001883000
O	1.225421000	-0.540504000	-0.027040000
H	0.443623000	-1.090003000	0.122322000
H	-0.578549000	0.415217000	0.058144000

O	-1.593363000	-0.145019000	0.101952000
H	-1.930732000	-0.124195000	-0.794825000

aINT1w: E= -357.246764

O	0.296725000	0.786860000	0.800316000
O	-0.005661000	1.319310000	-0.481665000
H	0.591236000	0.780452000	-1.045140000
O	1.336728000	-0.818459000	-0.591943000
N	0.909025000	-0.769065000	0.553105000
H	-1.367574000	-1.011999000	0.383984000
O	-2.112203000	-0.614981000	-0.087057000
H	-1.711546000	0.233167000	-0.327787000

aTS1w: E= -357.242381

O	-0.493729000	0.579549000	-0.816048000
O	0.085568000	1.383576000	0.380782000
H	-0.551084000	1.061588000	1.039171000
O	-1.467048000	-0.780882000	0.587120000
N	-0.733241000	-0.737273000	-0.433813000
H	1.425016000	-1.082511000	-0.209597000
O	2.188642000	-0.568934000	0.089661000
H	1.751294000	0.275359000	0.274999000

aINT2w: E= -357.299638

O	0.816047000	-1.204978000	0.001888000
O	-1.143108000	1.732475000	0.001240000
H	-0.210890000	1.329088000	0.000622000
O	1.335702000	0.843941000	-0.001679000

N	1.709848000	-0.354506000	-0.000299000
H	-1.120060000	-1.230568000	-0.000365000
O	-2.076632000	-1.061474000	-0.001216000
H	-2.094056000	-0.096693000	-0.000024000

aINT3w: E= -357.297743

N	0.835706000	-0.181776000	-0.142926000
O	2.010123000	0.110316000	-0.226530000
O	0.427498000	-1.223663000	0.332943000
O	-0.375969000	1.454884000	0.293986000
H	0.087159000	1.971116000	-0.373867000
H	-1.705833000	-1.032926000	-0.024105000
O	-2.364358000	-0.355318000	-0.214089000
H	-1.809622000	0.444489000	-0.092021000

aTS2w: E= -357.242072

N	0.830144000	-0.053624000	-0.079343000
O	2.024142000	-0.108719000	0.221010000
O	0.102909000	-1.067718000	-0.097611000
O	0.282878000	1.086153000	-0.275813000
H	-0.329322000	1.563490000	0.945250000
H	-1.766952000	-0.572456000	-0.077621000
O	-2.593934000	-0.083842000	0.072889000
H	-2.242685000	0.777336000	0.323972000

$HO_2^{\cdot}$: E= -150.875873

O	0.054937000	0.708060000	0.000000000
O	0.054937000	-0.598847000	0.000000000

H	-0.878989000	-0.873698000	0.000000000

bINT1: E= -280.753971

O	-1.316163000	0.729512000	-0.141354000
O	-1.555124000	-0.520725000	0.150265000
H	-0.690722000	-0.972404000	0.121018000
O	1.360877000	-0.486225000	-0.219735000
N	1.824858000	0.455988000	0.223653000

bTS1: E= -280.702997

O	-0.430289000	0.660063000	-0.229104000
O	-1.502285000	-0.393394000	0.160885000
H	-1.542410000	-0.872646000	-0.680794000
O	1.516100000	-0.445835000	-0.115762000
N	0.696314000	0.329426000	0.307520000

bINT2: E= -280.761594

O	-0.129013000	0.959953000	0.026994000
O	2.144836000	-0.441887000	0.013346000
H	2.462072000	0.476167000	0.049968000
O	-1.746208000	-0.500716000	0.065596000
N	-0.659856000	-0.087852000	-0.128207000

bINT2: E= -280.761594

O	-0.129013000	0.959953000	0.026994000
O	2.144836000	-0.441887000	0.013346000
H	2.462072000	0.476167000	0.049968000

O	-1.746208000	-0.500716000	0.065596000
N	-0.659856000	-0.087852000	-0.128207000

bINT3: E= -280.729310

N	-0.053921000	0.002269000	0.280900000
O	-0.684448000	1.064224000	-0.087887000
O	-0.756752000	-1.018140000	-0.057762000
O	1.264980000	-0.084142000	-0.169192000
H	1.787216000	0.288589000	0.552424000

bTS2: E= -280.651685

N	0.004478000	-0.000250000	-0.085362000
O	0.720696000	1.019963000	0.054926000
O	0.721786000	-1.019240000	0.055100000
O	-1.197682000	-0.000521000	-0.188528000
H	-1.989743000	0.000135000	1.225552000

HOONO: E= -280.784490

O	-0.526396000	0.721304000	-0.021700000
O	-1.259008000	-0.464299000	0.120271000
H	-1.397579000	-0.753180000	-0.792952000
O	1.195049000	-0.605074000	0.003096000
N	0.874346000	0.505390000	-0.002912000

bTS3: E= -280.753629

O	0.266571000	0.842271000	0.000008000
O	1.457878000	-0.534315000	0.000024000
H	2.206972000	0.081077000	-0.000181000
O	-1.240183000	-0.688484000	-0.000011000
N	-0.868729000	0.423306000	0.000001000

bTS4: E= -280.689612

N	-0.763089000	-0.081167000	0.006385000
O	-1.937195000	-0.098344000	0.108583000
O	0.116864000	0.665298000	0.019279000
O	1.396043000	-0.815905000	-0.274874000
H	2.362230000	-0.817537000	-0.362870000

$O_2^{\cdot -}$: E= -150.319462

O	0.000000000	0.000000000	0.660938000
O	0.000000000	0.000000000	-0.660938000

cINT1-A: E= -280.218384

O	1.003843000	0.638908000	0.000439000
O	1.319243000	-0.606306000	-0.000348000
O	-1.341907000	-0.552876000	0.000381000
N	-1.121348000	0.594598000	-0.000540000

cTS1-A: E= -280.171657

O	-0.464218000	0.593885000	-0.268929000
O	-1.549371000	-0.458800000	0.096203000

O	1.391629000	-0.498134000	-0.144772000
N	0.710811000	0.414913000	0.362855000

cINT2-A: E= -280.208045

O	0.056052000	1.020791000	-0.000067000
O	-1.764388000	-0.279182000	0.000028000
O	0.807109000	-0.960384000	-0.000054000
N	1.029974000	0.250029000	0.000107000

cINT1-B: E= -280.223113

O	-0.952703000	0.628898000	0.000004000
O	-1.316362000	-0.592441000	-0.000035000
O	1.328910000	-0.556270000	-0.000001000
N	1.074463000	0.594072000	0.000036000

cTS1-B: E= -280.221350

O	-0.773486000	0.611911000	0.000006000
O	-1.296186000	-0.559633000	-0.000035000
O	1.274502000	-0.559350000	0.000000000
N	0.908766000	0.579510000	0.000034000

$ONOO^-$: E= -280.236690

O	-0.564628000	0.637503000	0.000011000

O	-1.301392000	-0.537133000	-0.000037000
O	1.210340000	-0.572366000	0.000002000
N	0.749348000	0.539424000	0.000028000

cTS2-B: E= -280.201855

N	0.656480000	0.340777000	0.402566000
O	1.334663000	-0.428702000	-0.185545000
O	-0.519260000	0.640765000	-0.247295000
O	-1.389822000	-0.510243000	0.080594000

$O_2^{\cdot-}(H_2O)$: E= -226.752255

O	1.084896000	-0.626904000	-0.000002000
O	0.874347000	0.674283000	0.000003000
H	-0.846902000	0.517683000	-0.000018000
O	-1.692422000	-0.002567000	0.000000000
H	-1.287665000	-0.876180000	0.000017000

cINT1-Aw: E= -356.643489

O	-0.183136000	-0.573139000	-0.000017000
O	-0.355930000	0.709878000	0.000307000
O	2.305327000	0.488856000	-0.000263000
N	2.074251000	-0.644164000	0.000148000
H	-2.203736000	0.559615000	-0.000259000
O	-2.990113000	-0.023535000	-0.000125000
H	-2.525208000	-0.866946000	0.000007000

cTS1-Aw: E= -356.591113

O	0.146265000	-0.242173000	-0.210480000
O	-0.369230000	1.203476000	-0.044225000
O	2.179868000	-0.167805000	0.510360000
N	1.470960000	-0.341076000	-0.492614000
H	-2.121983000	0.364870000	0.143128000
O	-2.718736000	-0.401974000	0.154177000
H	-2.080075000	-1.109534000	0.026514000

cINT2-Aw: E= -356.630643

O	0.340866000	-0.582867000	-0.816179000
O	-0.309819000	1.542349000	-0.327691000
O	1.509997000	0.201568000	0.760215000
N	1.308696000	-0.702976000	-0.038880000
H	-1.755615000	0.362470000	0.395314000
O	-2.263977000	-0.463725000	0.377965000
H	-1.621790000	-1.020245000	-0.077634000

cINT1-Bw: E= -356.646360

O	0.141844000	-0.508451000	0.000031000
O	0.333241000	0.763463000	-0.000034000
O	-2.300248000	0.444033000	0.000062000
N	-1.971217000	-0.673165000	0.000107000
H	2.218095000	0.558415000	-0.000116000
O	2.965764000	-0.069068000	-0.000131000
H	2.455620000	-0.886075000	-0.000057000

cTS1-Bw: E= -356.642738

O	0.014979000	-0.425323000	0.000123000
O	-0.277671000	0.831198000	-0.000150000
O	2.240870000	0.359146000	-0.000286000
N	1.690820000	-0.691841000	-0.000038000
H	-2.109569000	0.489296000	0.000018000
O	-2.888305000	-0.101557000	0.000400000
H	-2.445152000	-0.954124000	-0.000448000

$ONOO^-(H_2O)$: E= -356.663761

O	-0.195561000	-0.494875000	0.002324000
O	0.302071000	0.808633000	0.008029000
O	-2.156577000	0.371138000	-0.003024000
N	-1.510508000	-0.634381000	-0.003318000
H	1.908653000	0.381101000	-0.009153000
O	2.811104000	-0.054658000	-0.009540000
H	2.576605000	-0.982339000	0.050068000